



北京大學

PEKING UNIVERSITY

The Seventh International Symposium on Chiral Symmetry in Hadrons and Nuclei,

27 – 30 October, 2013, Beijing, China

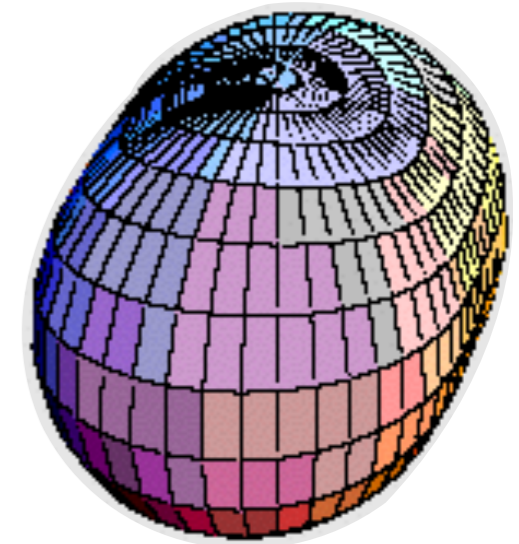
Antimagnetic rotation in nuclei: A microscopic description

Pengwei Zhao

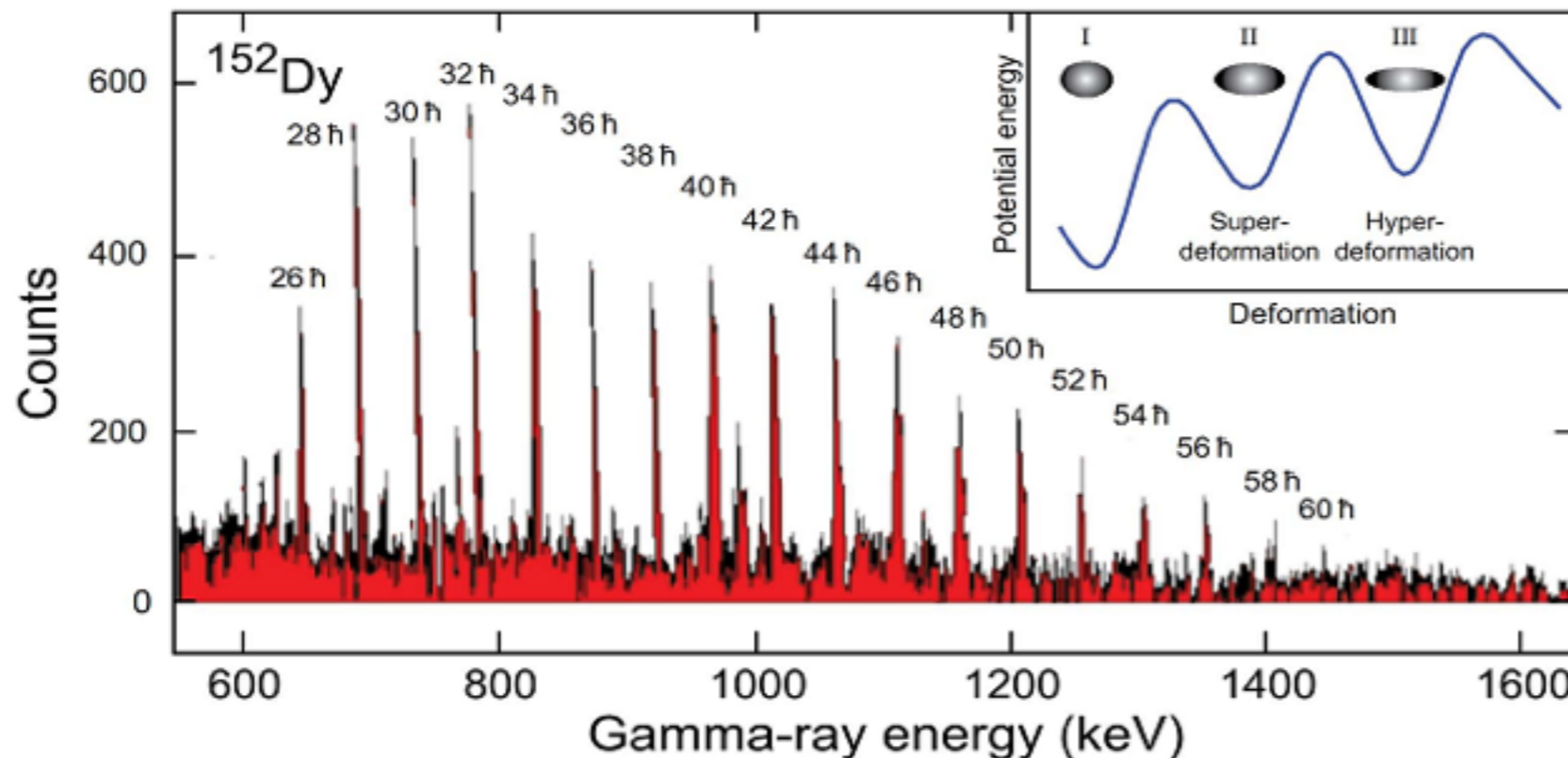
School of Physics, Peking University

Rotation bands in nuclei

- Substantial quadrupole deformation
- Strong electric quadrupole (E2) transitions
- Rotational bands with $\Delta I = 2$
- Coherent collective rotation of many nucleons



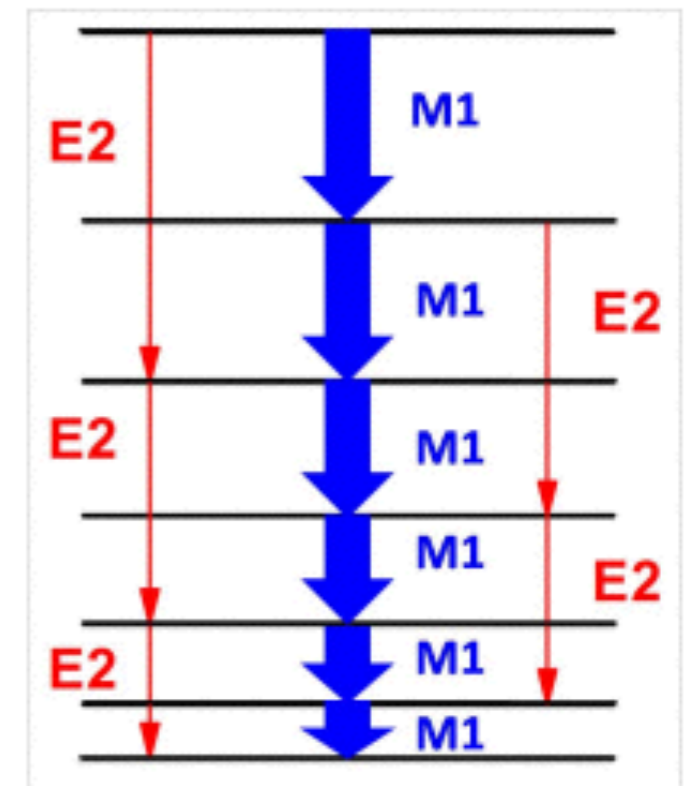
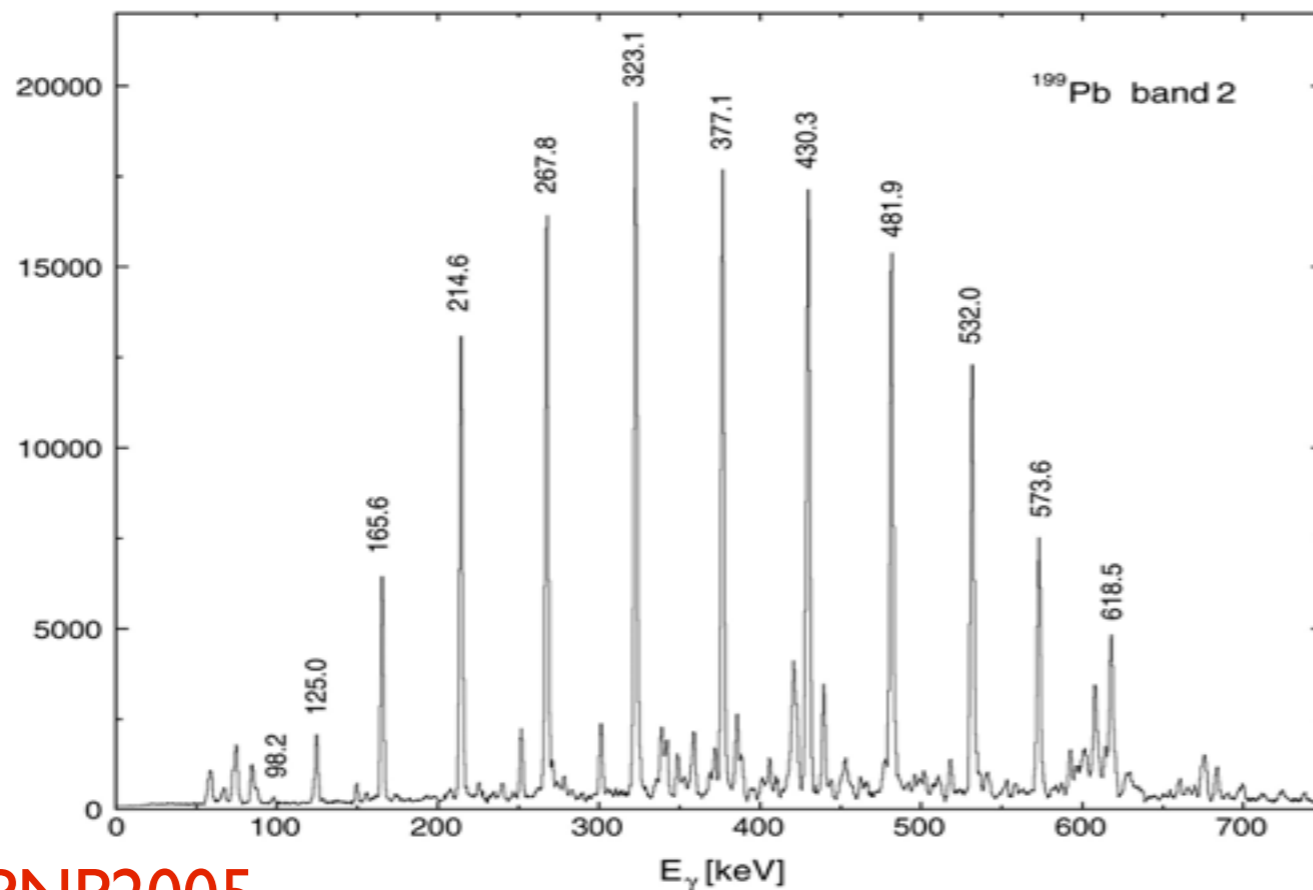
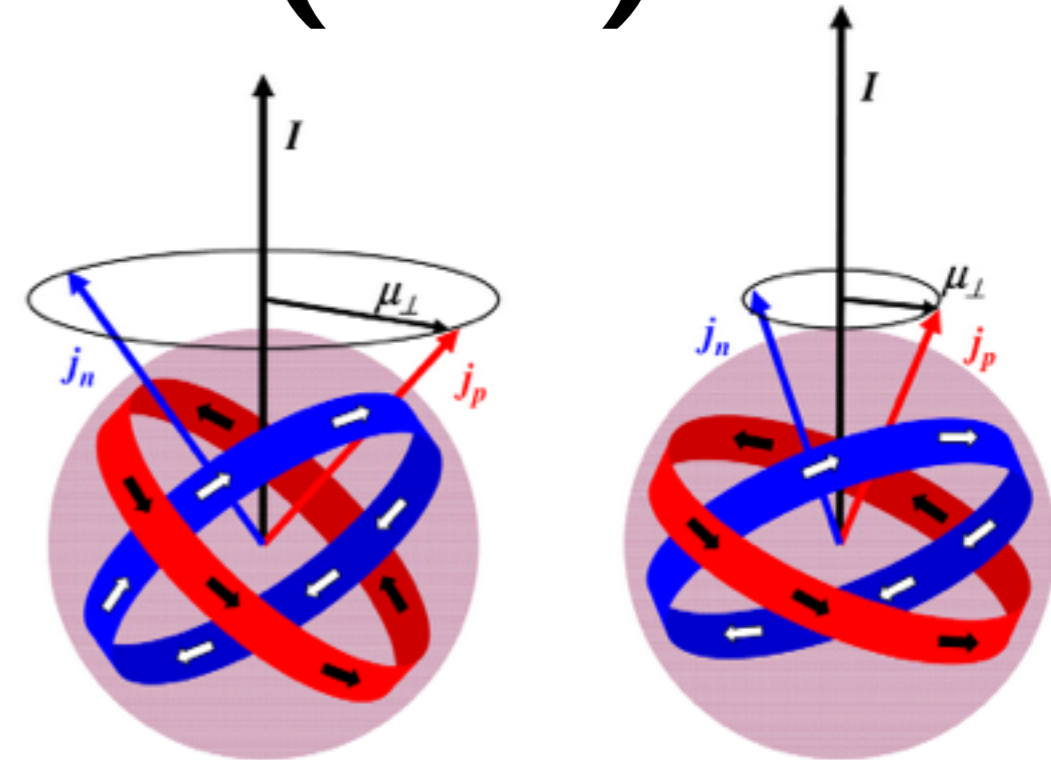
Bohr PR 1951



Twin PRL 1986

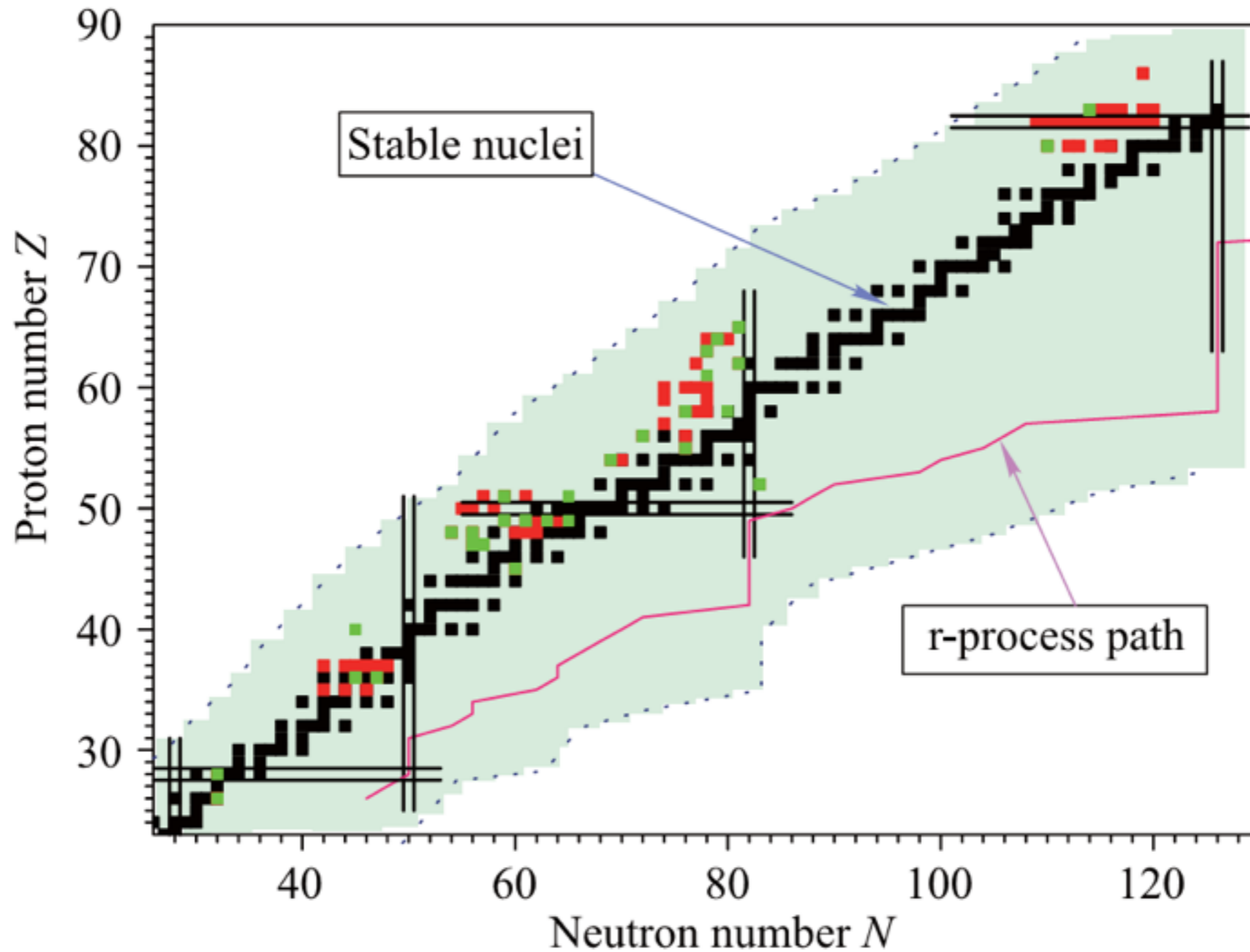
Magnetic Rotation (MR)

- near-spherical or weakly deformed nuclei
- strong M1 and very weak E2 transitions
- rotational bands with $\Delta I = 1$
- shears mechanism



Experiment: MR

Magnetic rotation: 85 nuclei

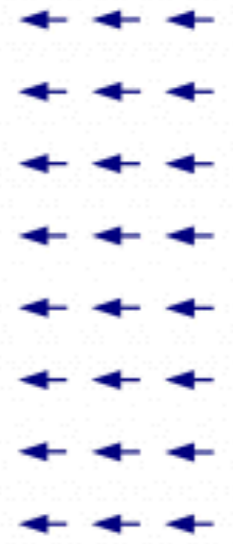
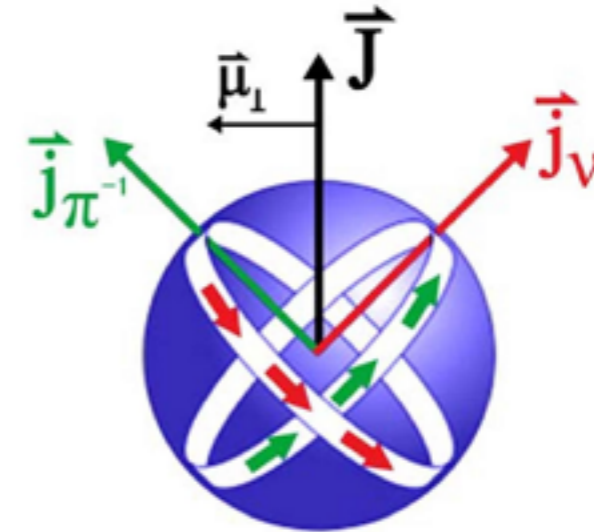


Meng, Peng, Zhang, PWZ, Front. Phys. 8, 55 (2013)

Antimagnetic Rotation (AMR)

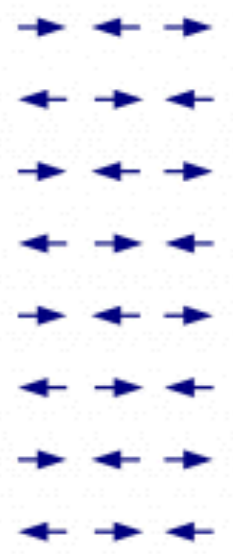
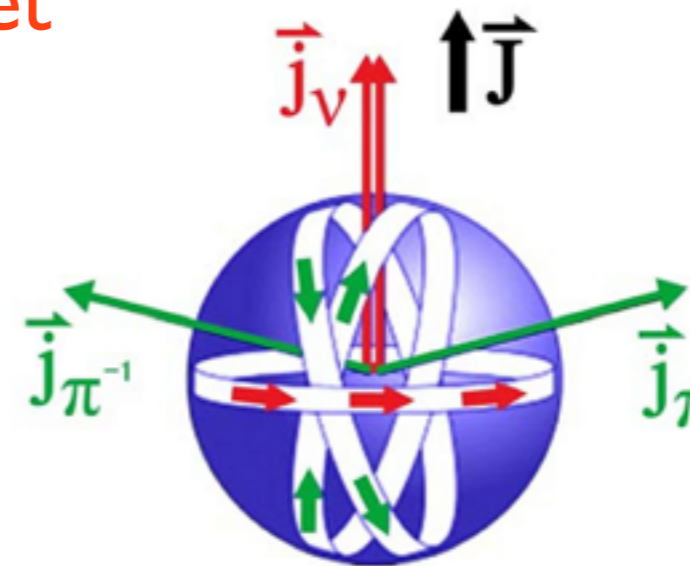
Magnetic rotation \longleftrightarrow Ferromagnet

- ✓ rotational bands with $\Delta I = 1$
- ✓ near spherical nuclei; weak E2 transitions
- ✓ strong M1 transitions
- ✓ $B(M1)$ decrease with spin
- ✓ shears mechanism



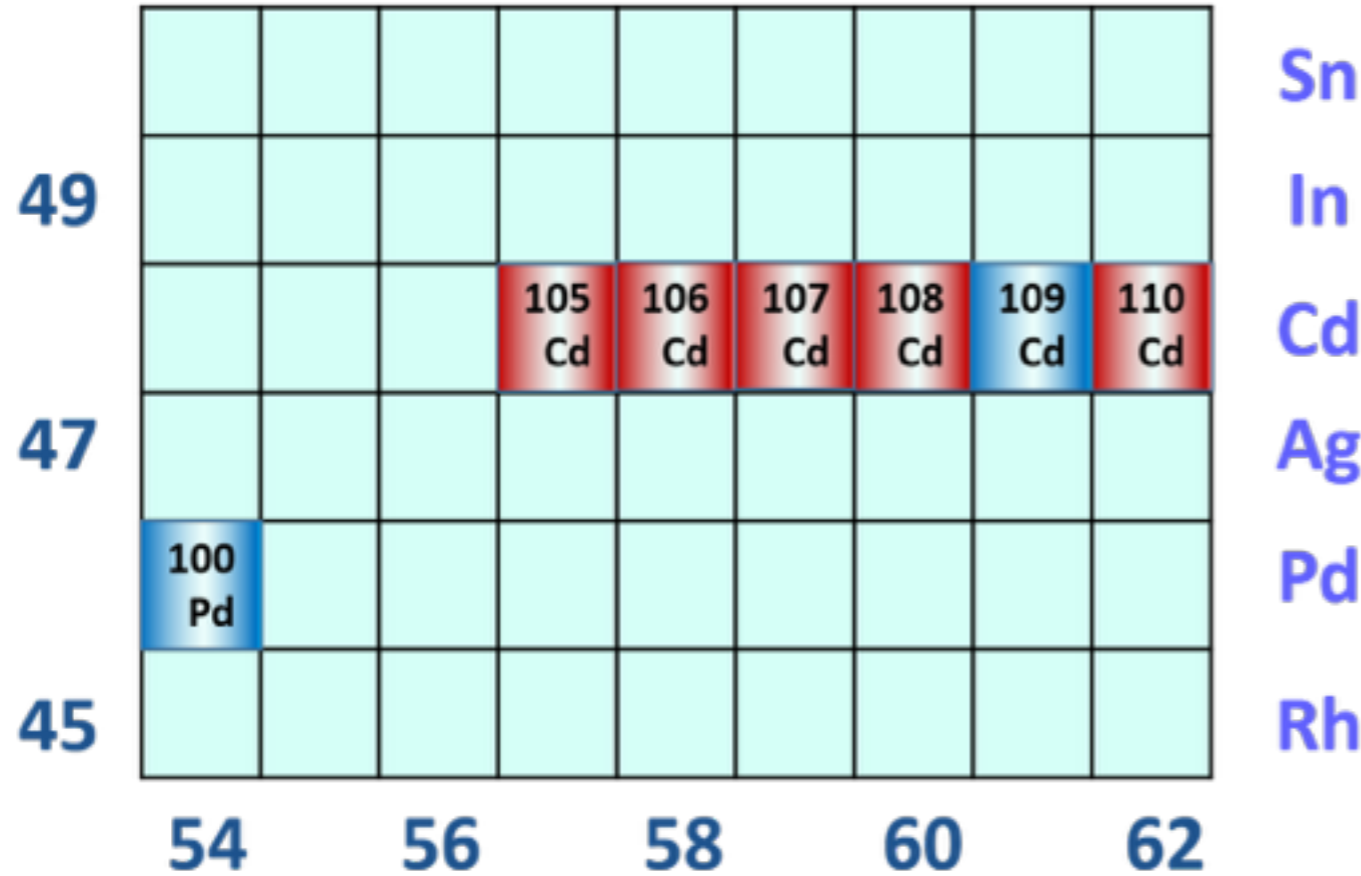
Antimagnetic rotation \longleftrightarrow Antiferromagnet

- ✓ rotational bands with $\Delta I = 2$
- ✓ near spherical nuclei; weak E2 transitions
- ✓ no M1 transitions
- ✓ $B(E2)$ decrease with spin
- ✓ two “shears-like” mechanism

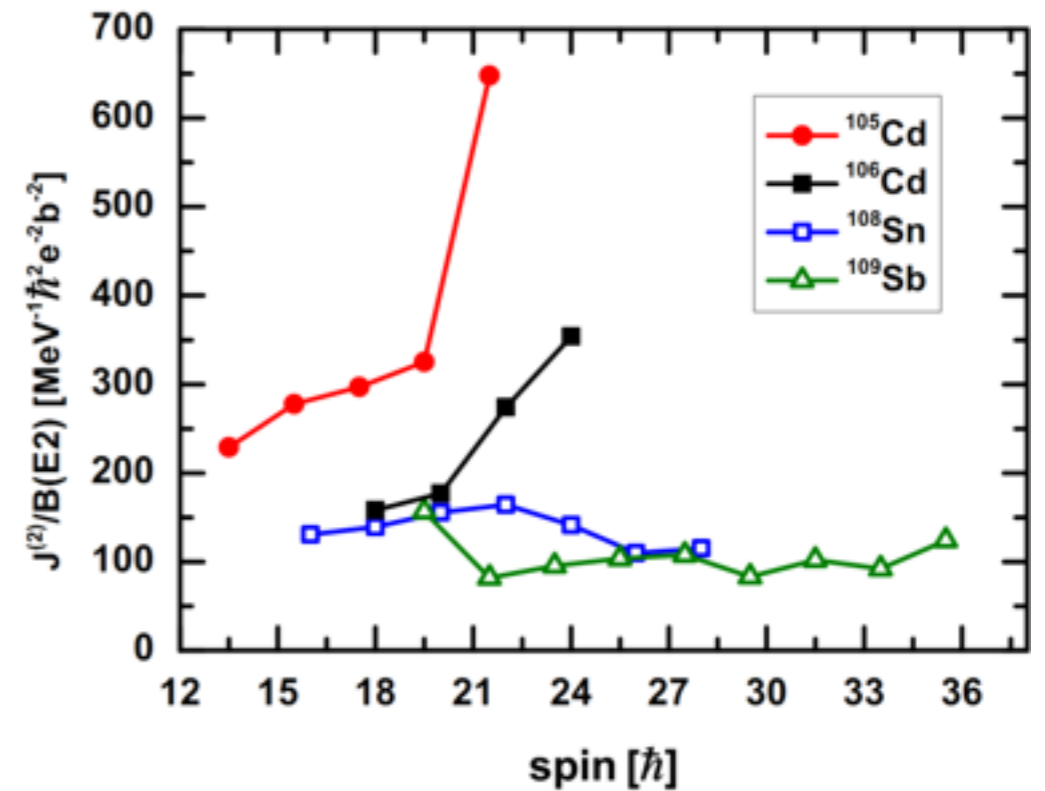
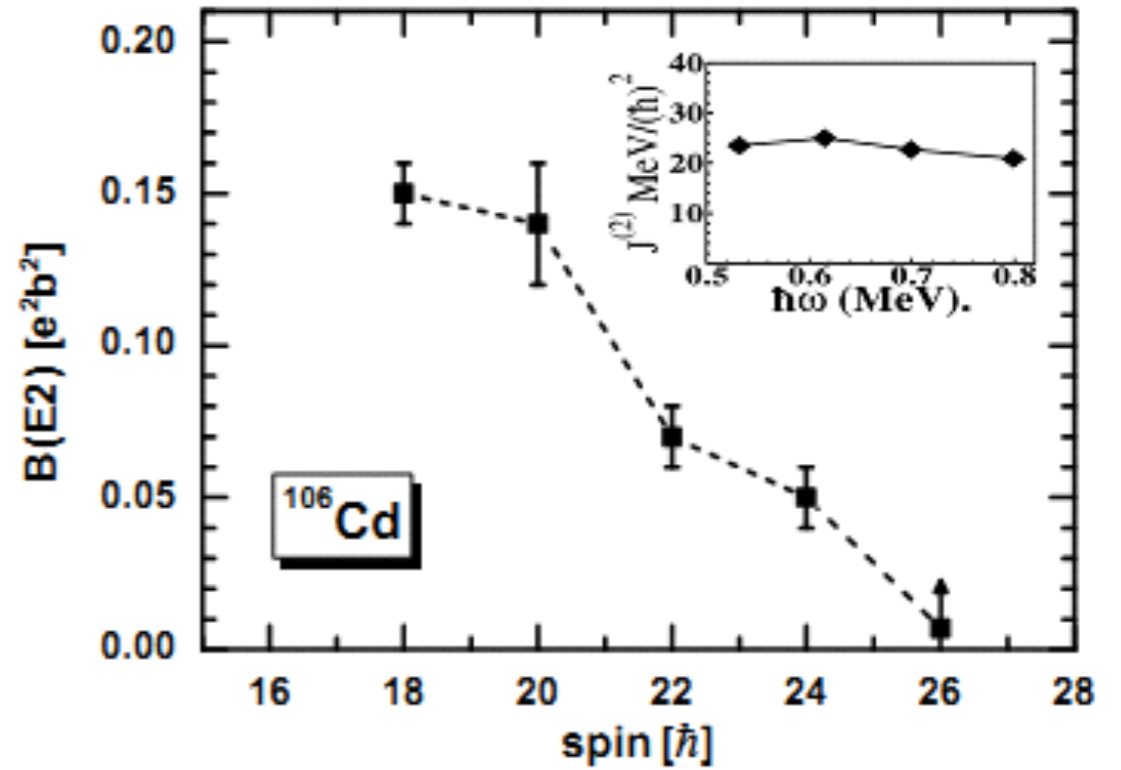


Experiment: AMR

$A \sim 100$



Small $B(E2)$
 Decrease tendency
 Large $J(2)/B(E2)$
 Increase tendency

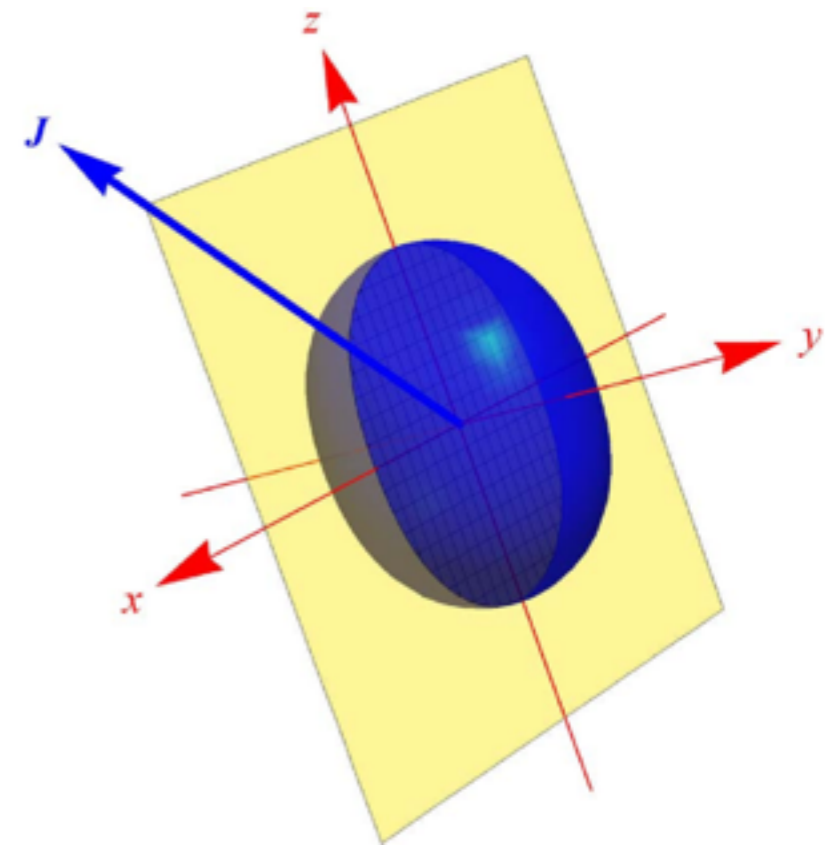


Simons PRL2003; Simons PRC2005

Theory

- ✓ Semiclassical particle plus rotor model [Clark ARNPS2000](#)
simple geometry for the energies and transition probabilities
- ✓ Pairing-plus-quadrupole tilted axis cranking (TAC) model
a schematic Hamiltonian [Frauendorf NPA 1993](#); [Frauendorf NPA2000](#)

A fully self-consistent microscopic investigation?



DFT: Cranking version

- **TAC based on Covariant Density Functional Theory**

Meson exchange version:

3-D Cranking: *Madokoro, Meng, Matsuzaki, Yamaji, PRC 62, 061301 (2000)*

2-D Cranking: *Peng, Meng, Ring, Zhang, PRC 78, 024313 (2008)*

Point-coupling version: Simple and more suitable for systematic investigations

2-D Cranking: *PWZ, Zhang, Peng, Liang, Ring, Meng, PLB 699, 181 (2011)*

- **TAC based on Skyrme Density Functional Theory**

3-D Cranking: *Olbratowski, Dobaczewski, Dudek, Płóciennik, PRL 93, 052501(2004)*

2-D Cranking: *Olbratowski, Dobaczewski, Dudek, Rzaca-Urban, Marcinkowska, Lieder, APPB 33, 389(2002)*

Fully self-consistent microscopic investigations

- fully taken into account polarization effects
- self-consistently treated the nuclear currents
- without any adjustable parameters for rotational excitations

Tilted axis cranking CDFT

General Lagrangian density

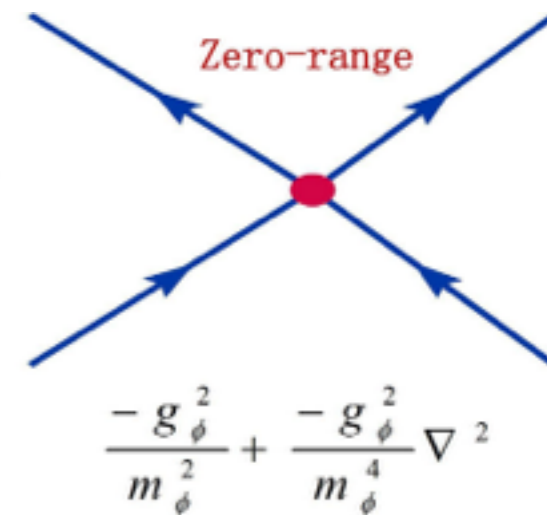
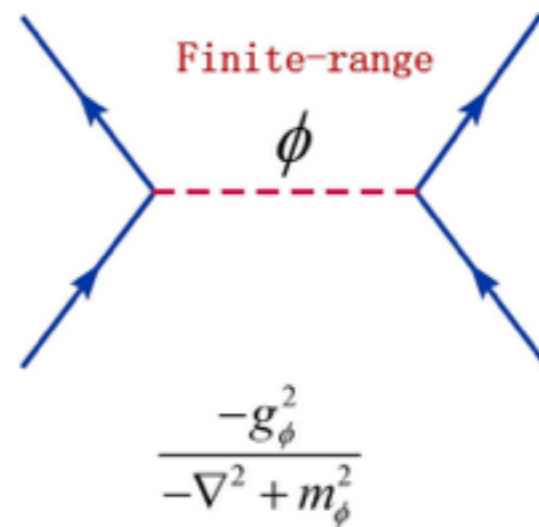
$$L = \bar{\psi} (i\gamma_\mu \partial^\mu - m)\psi$$

$$-\frac{1}{2}\alpha_S (\bar{\psi}\psi)(\bar{\psi}\psi) - \frac{1}{2}\alpha_V (\bar{\psi}\gamma_\mu\psi)(\bar{\psi}\gamma^\mu\psi)$$

$$-\frac{1}{2}\alpha_{TV} (\bar{\psi}\tau\gamma_\mu\psi)(\bar{\psi}\tau\gamma^\mu\psi) - \frac{1}{3}\beta_S (\bar{\psi}\psi)^3 - \frac{1}{4}\gamma_S (\bar{\psi}\psi)^4$$

$$-\frac{1}{4}\gamma_V [(\bar{\psi}\gamma_\mu\psi)(\bar{\psi}\gamma^\mu\psi)]^2 - \frac{1}{2}\delta_S \partial_\nu (\bar{\psi}\psi) \partial^\nu (\bar{\psi}\psi) - \frac{1}{2}\delta_V \partial_\nu (\bar{\psi}\gamma_\mu\psi) \partial^\nu (\bar{\psi}\gamma^\mu\psi) - \frac{1}{2}\delta_{TV} \partial_\nu (\bar{\psi}\tau\gamma_\mu\psi) \partial^\nu (\bar{\psi}\tau\gamma_\mu\psi)$$

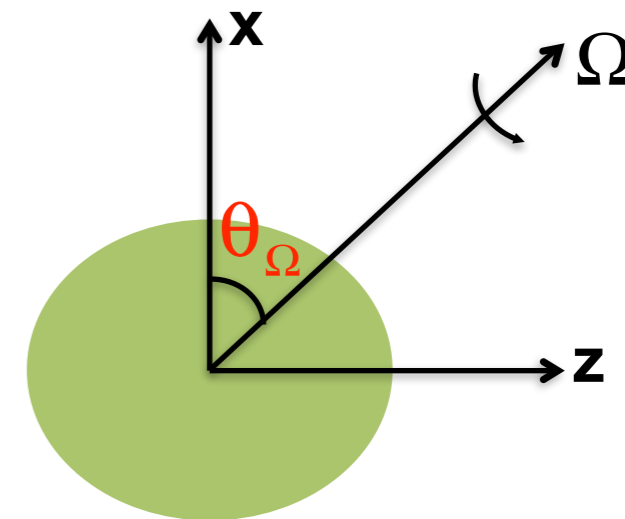
$$-e \frac{1-\tau_3}{2} \bar{\psi}\gamma^\mu\psi A_\mu - \frac{1}{4} F^{\mu\nu} F_{\mu\nu}$$



Transformed to the frame rotating with the uniform velocity

$$\Omega = (\Omega_x, 0, \Omega_z) = (\Omega \cos\theta_\Omega, 0, \Omega \sin\theta_\Omega)$$

$$x^\alpha = \begin{pmatrix} t \\ \mathbf{x} \end{pmatrix} \rightarrow \tilde{x}^\alpha = \begin{pmatrix} \tilde{t} \\ \tilde{\mathbf{x}} \end{pmatrix} = \begin{pmatrix} 1 & 0 \\ 0 & \mathbf{R} \end{pmatrix} \begin{pmatrix} t \\ \mathbf{x} \end{pmatrix}$$



Equation of motion

Dirac equation

$$\begin{pmatrix} m + \mathbf{S} + \mathbf{V} - \boldsymbol{\Omega} \cdot \mathbf{J} & \sigma(p - \mathbf{V}) \\ \sigma(p - \mathbf{V}) & -m - \mathbf{S} + \mathbf{V} - \boldsymbol{\Omega} \cdot \mathbf{J} \end{pmatrix} \begin{pmatrix} f \\ g \end{pmatrix} = \varepsilon \begin{pmatrix} f \\ g \end{pmatrix}$$

$$\mathbf{V}(r) = \alpha_V \rho_V + \gamma_V \rho_V^3 + \delta_V \Delta \rho_V + \tau_3 \alpha_{TV} \rho_{TV} + \tau_3 \delta_{TV} \Delta \rho_{TV} + e \frac{1 - \tau_3}{2} A$$

$$\mathbf{V}(r) = \alpha_V \mathbf{j}_V + \gamma_V \mathbf{j}_V^3 + \delta_V \Delta \mathbf{j}_V + \tau_3 \alpha_{TV} \mathbf{j}_{TV} + \tau_3 \delta_{TV} \Delta \mathbf{j}_{TV} + e \frac{1 - \tau_3}{2} \mathbf{A}$$

$$\mathbf{S}(r) = \alpha_S \rho_S + \beta_S \rho_S^2 + \gamma_S \rho_S^3 + \delta_S \Delta \rho_S$$

$\mathbf{V}(r)$ vector potential time-like

$\mathbf{V}(r)$ vector potential space-like

$\mathbf{S}(r)$ scalar potential

Observables

Binding energy

$$\begin{aligned} E_{\text{tot}} = & \sum_{k=1}^A \epsilon_k - \int d^3r \left\{ \frac{1}{2} \alpha_S \rho_S^2 + \frac{1}{2} \alpha_V j_V^\mu (j_V)_\mu \right. \\ & + \frac{1}{2} \alpha_{TV} j_{TV}^\mu (j_{TV})_\mu + \frac{2}{3} \beta_S \rho_S^3 + \frac{3}{4} \gamma_S \rho_S^4 \\ & + \frac{3}{4} \gamma_V (j_V^\mu (j_V)_\mu)^2 + \frac{1}{2} \delta_S \rho_S \Delta \rho_S + \frac{1}{2} \delta_V (j_V)_\mu \Delta j_V^\mu \\ & \left. + \frac{1}{2} \delta_{TV} j_{TV}^\mu \Delta (j_{TV})_\mu + \frac{1}{2} e j_p^0 A_0 \right\} + \sum_{k=1}^A \langle k | \boldsymbol{\Omega} \hat{\mathbf{J}} | k \rangle \\ & + E_{\text{c.m.}} \end{aligned}$$

Angular momentum

$$J = \sqrt{\langle \hat{J}_x \rangle^2 + \langle \hat{J}_z \rangle^2} \equiv \sqrt{I(I+1)}$$

Observables

Binding energy

$$E_{\text{tot}} = \sum_{k=1}^A \epsilon_k - \int d^3r \left\{ \frac{1}{2} \alpha_S \rho_S^2 + \frac{1}{2} \alpha_V j_V^\mu (j_V)_\mu \right. \\ + \frac{1}{2} \alpha_{TV} j_{TV}^\mu (j_{TV})_\mu + \frac{2}{3} \beta_S \rho_S^3 + \frac{3}{4} \gamma_S \rho_S^4 \\ + \frac{3}{4} \gamma_V (j_V^\mu (j_V)_\mu)^2 + \frac{1}{2} \delta_S \rho_S \Delta \rho_S + \frac{1}{2} \delta_V (j_V)_\mu \Delta j_V^\mu \\ \left. + \frac{1}{2} \delta_{TV} j_{TV}^\mu \Delta (j_{TV})_\mu + \frac{1}{2} e j_p^0 A_0 \right\} + \sum_{k=1}^A \langle k | \boldsymbol{\Omega} \hat{\mathbf{J}} | k \rangle \\ + E_{\text{c.m.}}$$

Angular momentum

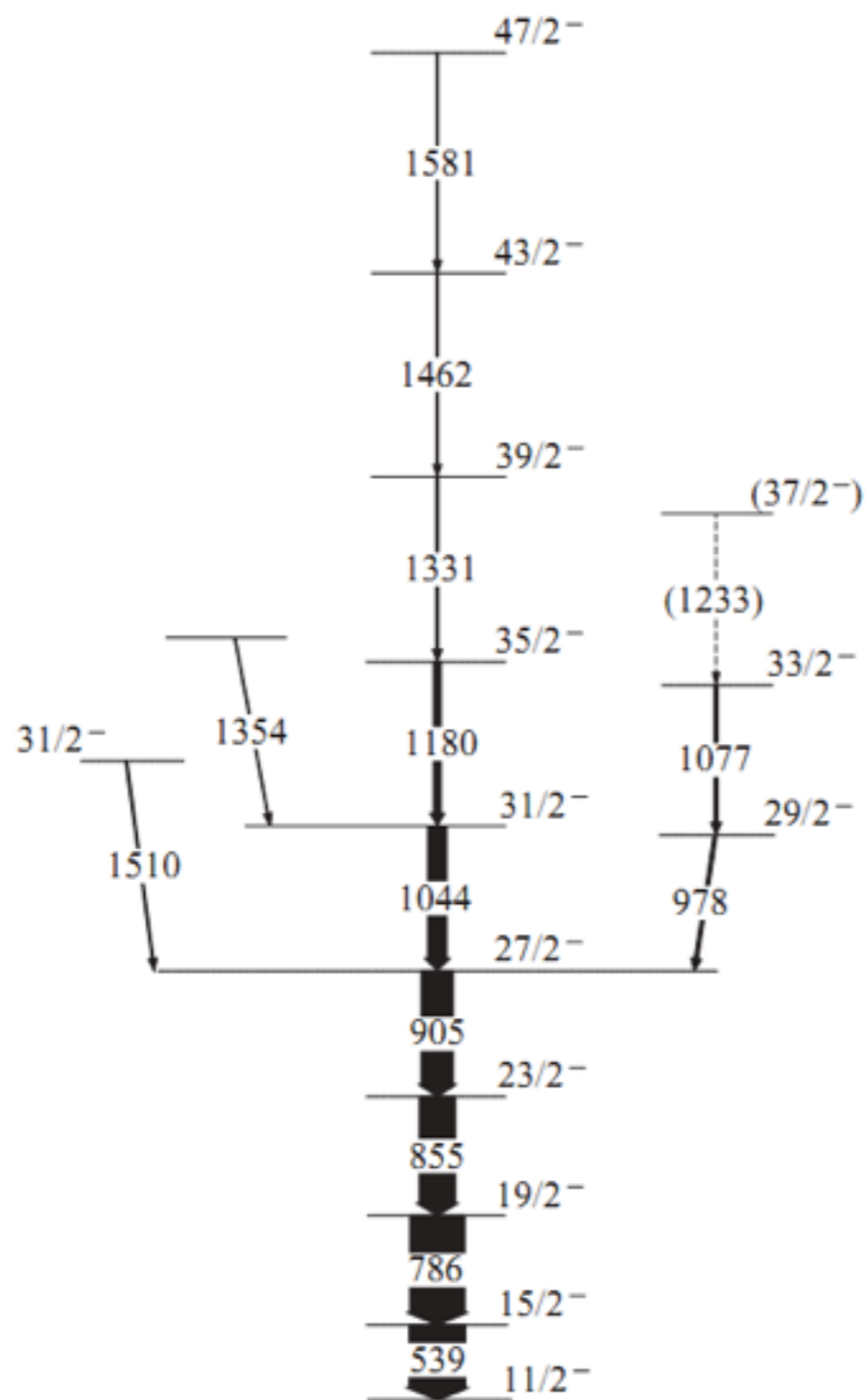
$$J = \sqrt{\langle \hat{J}_x \rangle^2 + \langle \hat{J}_z \rangle^2} \equiv \sqrt{I(I+1)}$$

B(M1) and B(E2) transition probabilities

$$B(M1) = \frac{3}{8\pi} \mu_\perp^2 = \frac{3}{8\pi} (\mu_x \sin \theta_J - \mu_z \cos \theta_J)^2, \\ B(E2) = \frac{3}{8} \left[Q_{20}^p \cos^2 \theta_J + \sqrt{\frac{2}{3}} Q_{22}^p (1 + \sin^2 \theta_J) \right]^2,$$

AMR in ^{105}Cd

First odd-A nucleus with antimagnetic rotation

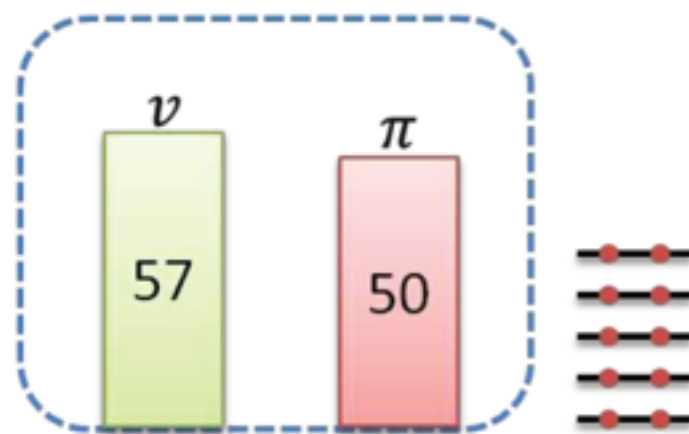


Choudhury et al, PRC 82 , 061308 (2010)

Numerical Details

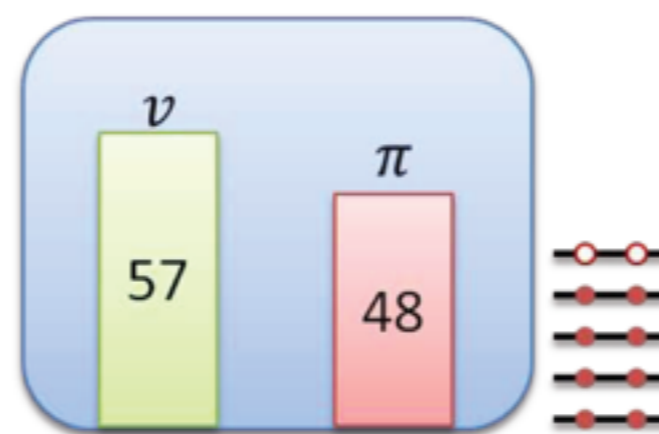
- ✓ Harmonic oscillator shells: $N_f = 10$
- ✓ Effective interaction: PC-PK1
- ✓ Configurations: $\nu[h_{11/2}(g_{7/2})^2] \otimes \pi[(g_{9/2})^{-2}]$
- ✓ Polarizations:

Without Polarization
Self-consistency



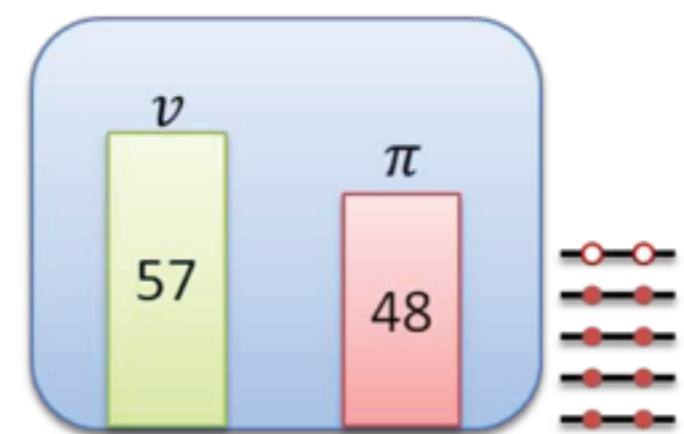
^{107}Sn

Without Polarization
Without Self-consistency



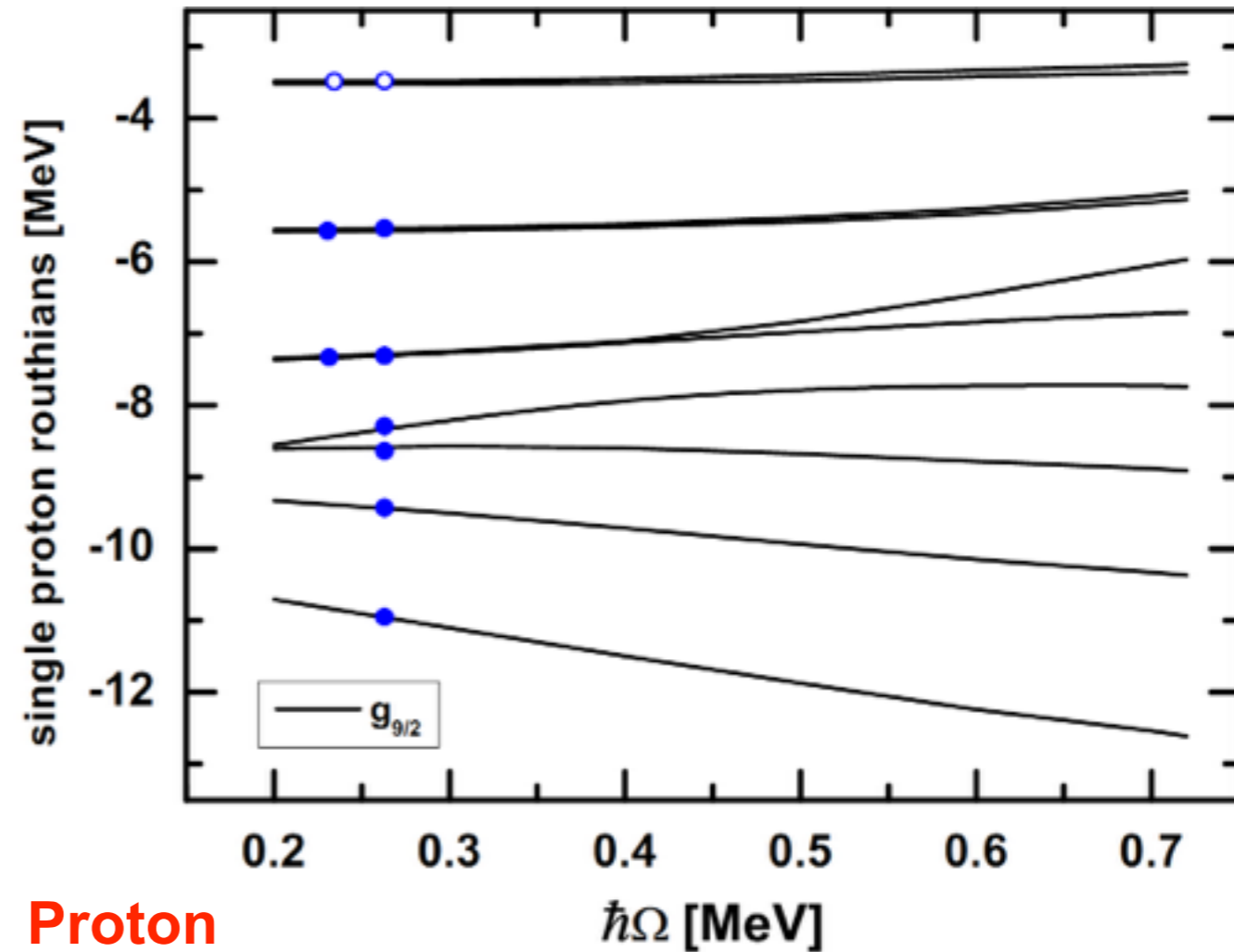
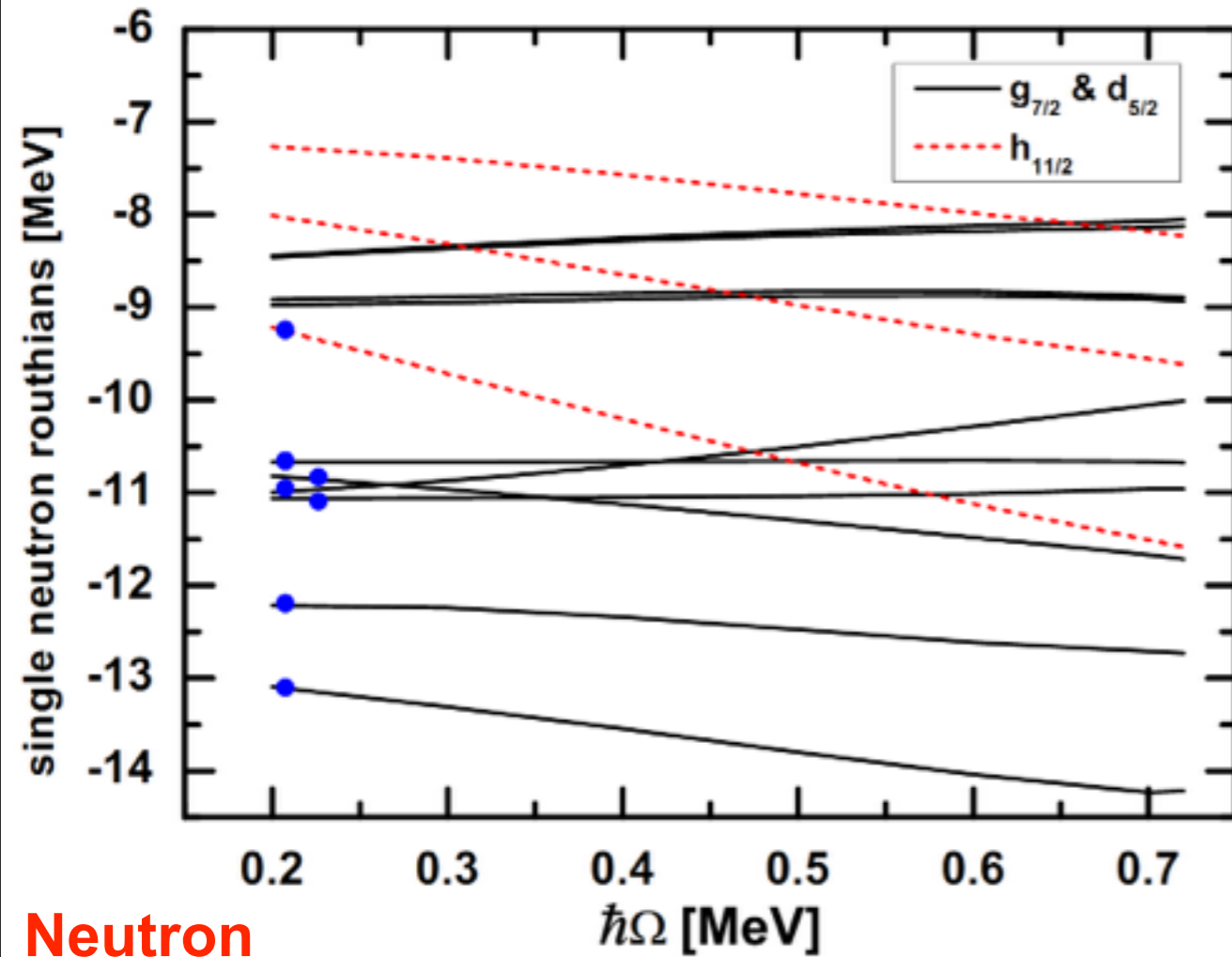
$^{107}\text{Sn} + \pi[(g_{9/2})^{-2}]$

With Polarization
Self-consistency



^{105}Cd

Single particle routhians

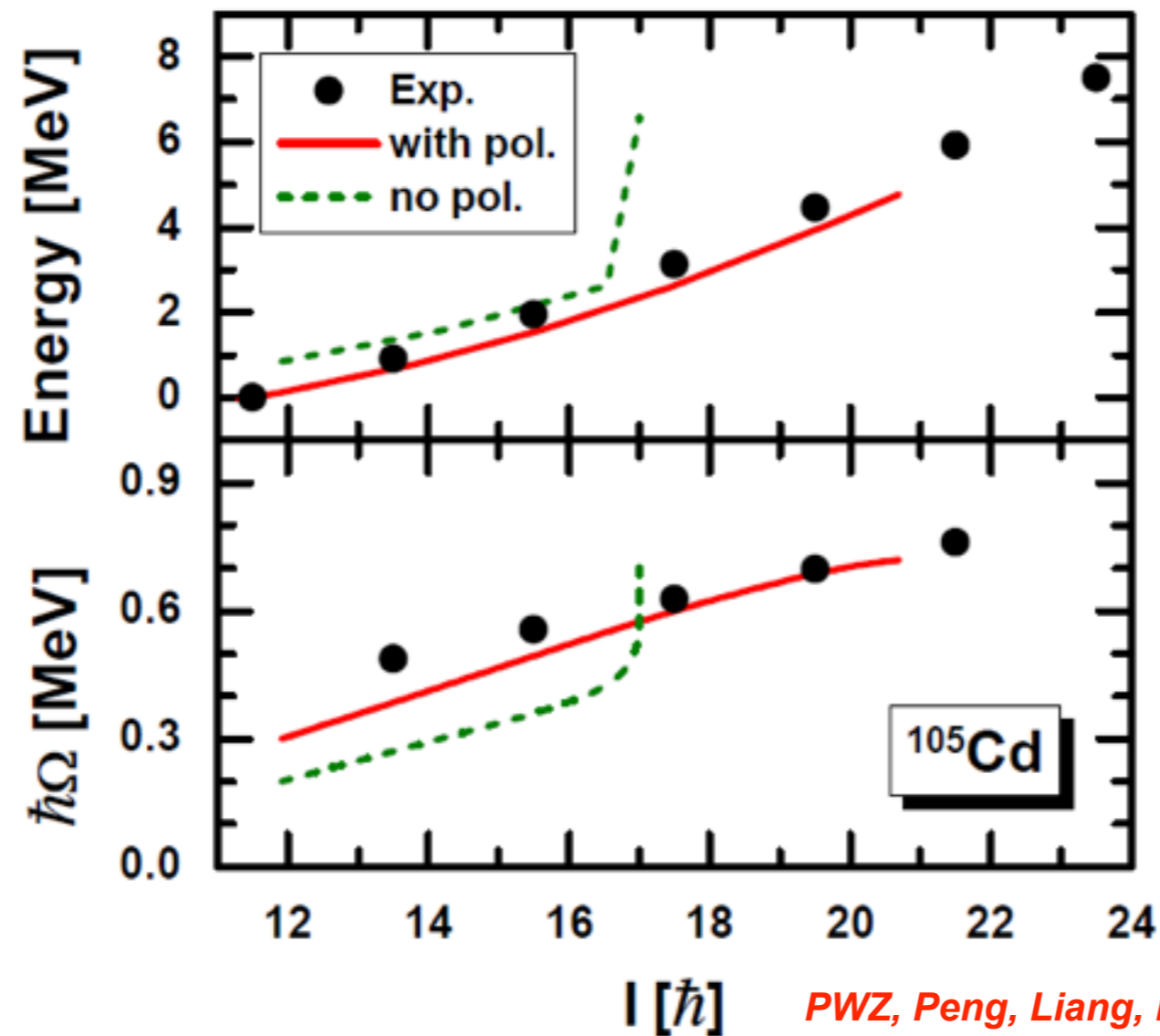


Neutron

Proton

- ✓ Time reversal symmetry broken: energy splitting
- ✓ For proton, two holes in the top of $g_{9/2}$ shell
- ✓ For neutron, one particle in the bottom of $h_{11/2}$ shell, the other six are distributed over the (gd) shell with strong mixing
- ✓ This configuration is similar to $\nu[h_{11/2}(g_{7/2})^2] \otimes \pi[(g_{9/2})^{-2}]$, but not exactly

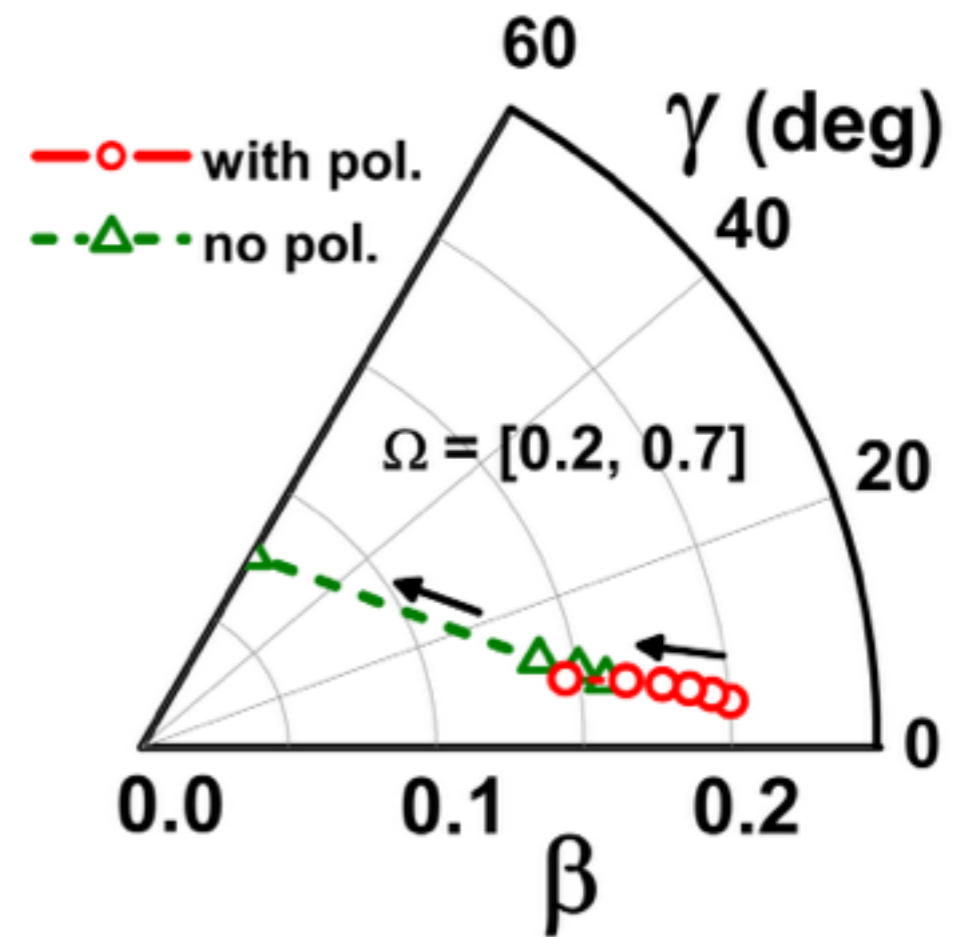
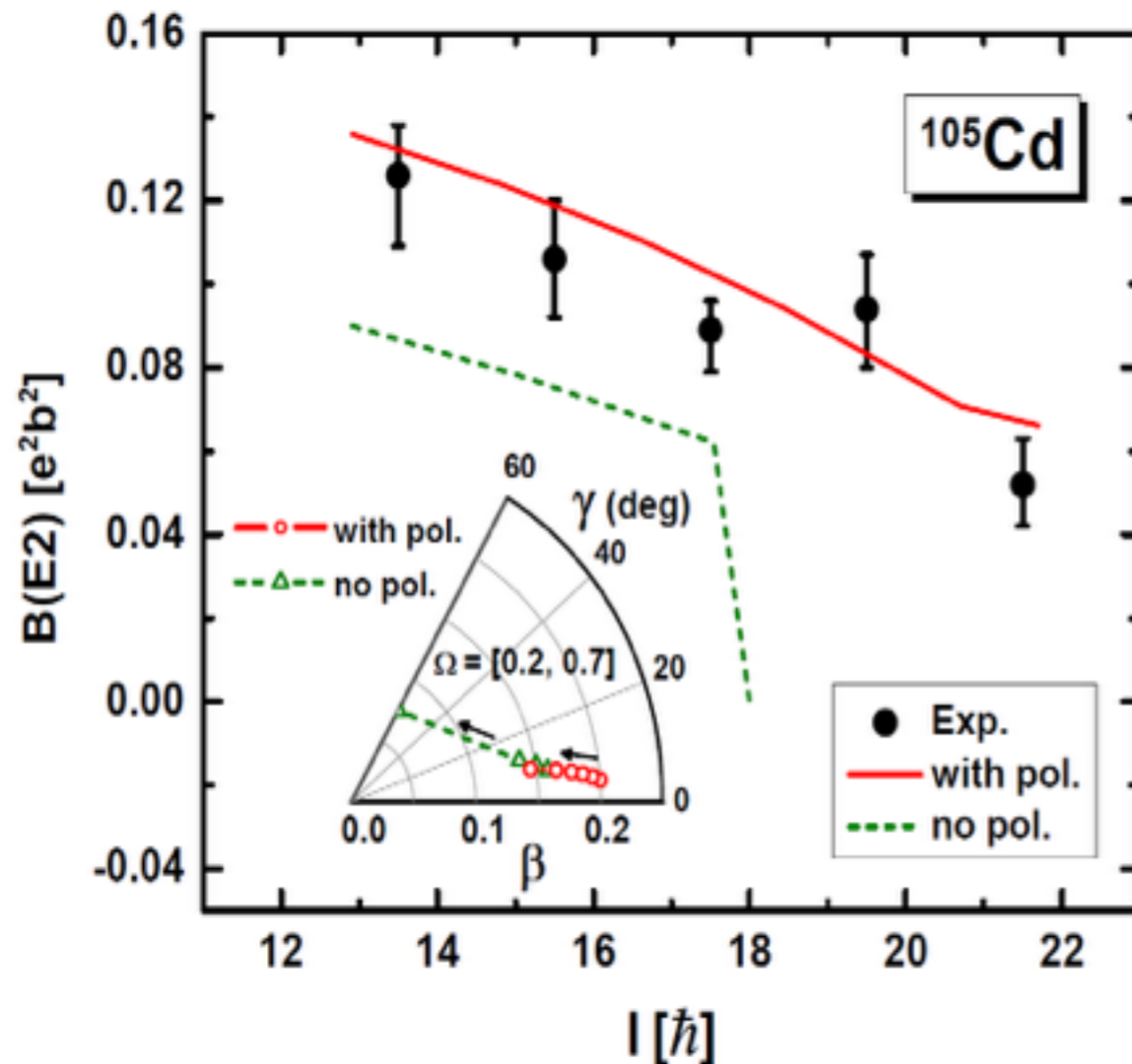
Energy and angular momentum



PWZ, Peng, Liang, Ring, Meng PRL 107, 122501(2011)

- ✓ The energy and total angular momentum agree well with the data.
- ✓ The spin increase linearly with frequency / nearly constant moment of inertia.
- ✓ Without polarization, a much smaller frequency is needed to reach the same angular momentum.
- ✓ Without polarization, there is a maximal angular momentum of roughly $17\hbar$

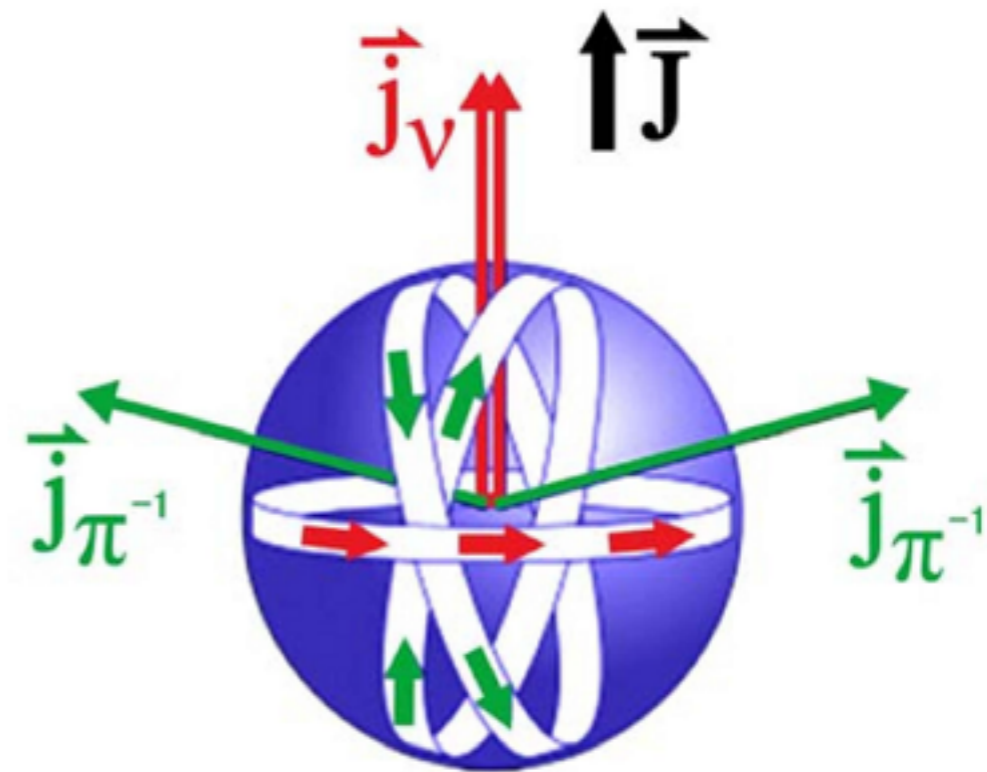
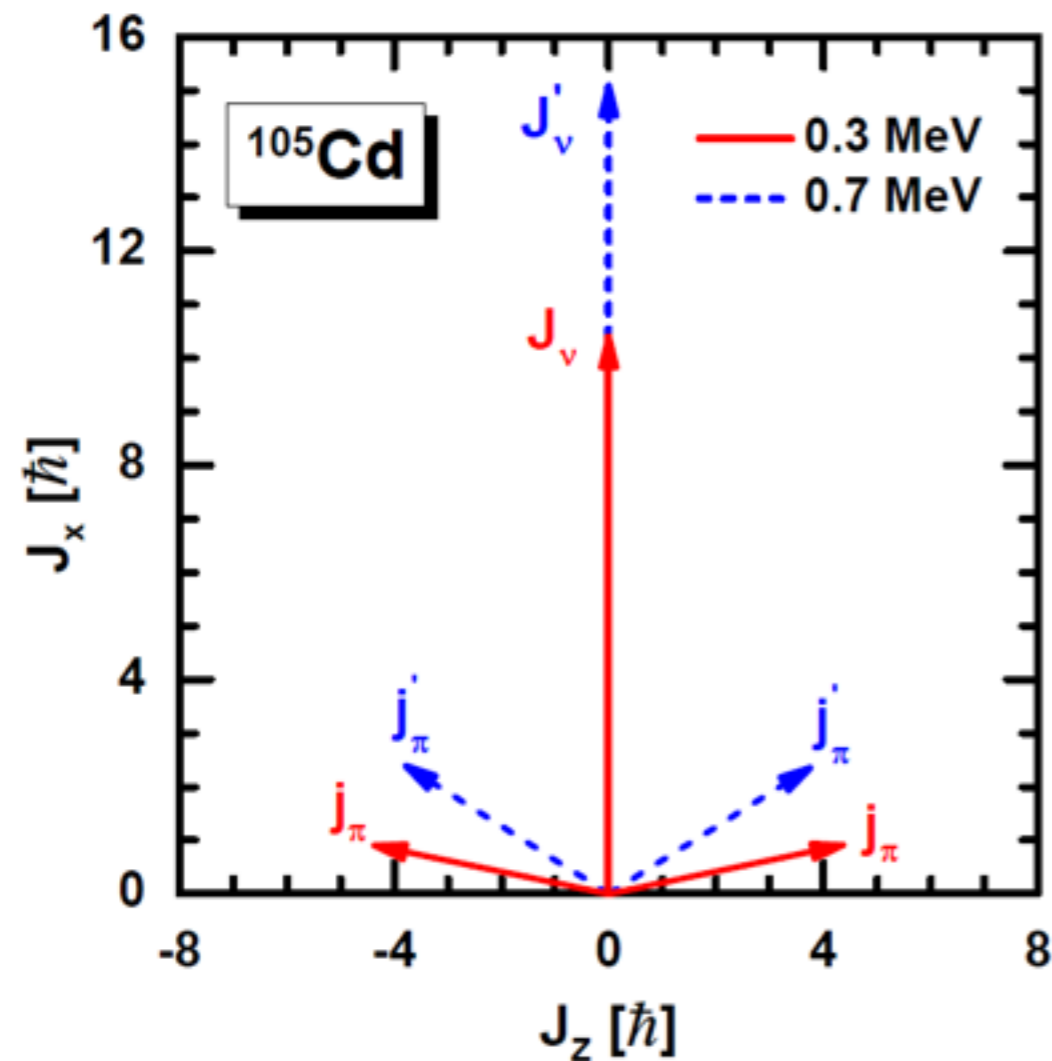
B(E2) and deformation



PWZ, Peng, Liang, Ring, Meng PRL 107, 122501(2011)

- ✓ The calculated $B(E2)$ values are in excellent agreement with the data.
- ✓ The $B(E2)$ values decrease with the increasing spin / two “shears-like” mechanism.
- ✓ Without polarization, the $B(E2)$ values are reduced to only ~60% of the self-consistent results, and dropped to zero when the frequency $\Omega \geq 0.5$ MeV.
- ✓ It is of importance to emphasize that polarization effects play a very important role in the self-consistent microscopic description of AMR bands, especially for the E2 transitions.

Two shears mechanism



PWZ, Peng, Liang, Ring, Meng PRL 107, 122501(2011)

- ✓ The two proton angular momentum are pointing opposite to each other and are nearly perpendicular to the neutron angular momentum. They form the blades of the two shears.
- ✓ Increasing Ω , the two proton blades towards to each other and generates the total angular momentum.

Summary

- Covariant density functional theory has been extended to describe rotational excitations including MR and AMR.
- ^{105}Cd : AMR
reproduce well the AMR pictures, E, I, and B(E2) values in a fully self-consistent microscopic way for the first time

In collaboration with

Haozhao Liang

Jie Meng

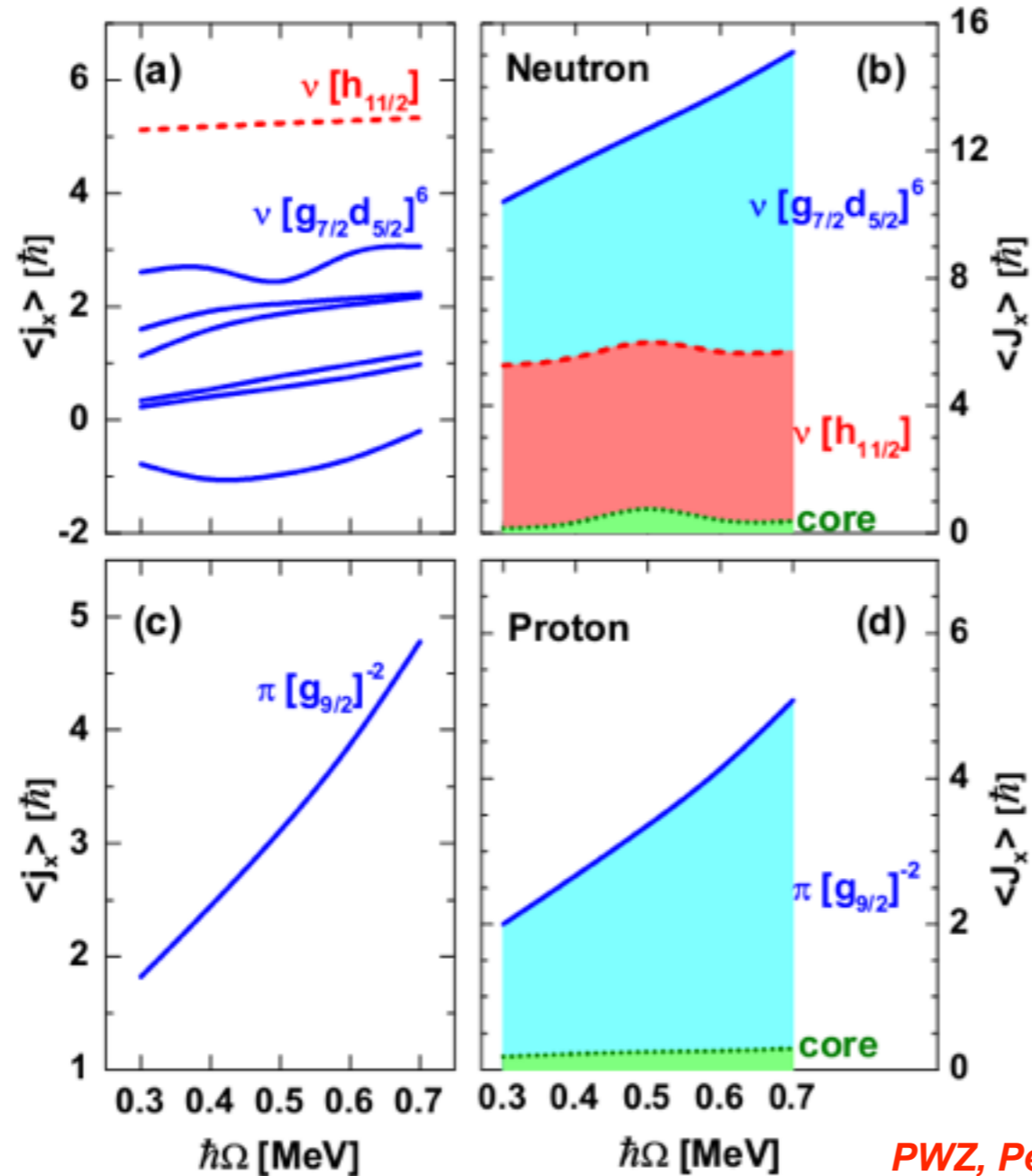
Jing Peng

Peter Ring

Shuangquan Zhang

Thank You!

Single-particle angular momentum



PWZ, Peng, Liang, Ring, Meng PRC 85, 054310 (2012)

- ✓ For the protons, only the two holes in the $g_{9/2}$ shell contribute.
- ✓ For the neutrons, only the particles above the $N=50$ shell contribute.
- ✓ Angular momentum results from the alignment of proton holes and the mixing within the neutron orbitals.
- ✓ Due to the strong mixing between neutrons, a core in the phenomenological model cannot be well defined.